Spectral analysis, DFT calculations on molecular structure, NBO, NLO and thermodynamic properties, multiple interactions and AIM approach of 4-(4-nitrophenyl)-2-oxo-7-phenyl-2,3,4,5,6,7-hexahydro-1H-pyrrolo [2,3-d] pyrimidine-5-carboxylic acid

By

Huda Parveen, Abha Bishnoi, Shaheen Fatma and Poornima Devi

ISSN 2319-3077 Online/Electronic
ISSN 0970-4973 Print

UGC Approved Journal No. 62923
MCI Validated Journal
Index Copernicus International Value
IC Value of Journal 82.43 Poland, Europe (2016)
Journal Impact Factor: 4.275
Global Impact factor of Journal: 0.876
Scientific Journals Impact Factor: 3.285
InfoBase Impact Factor: 3.66

J. Biol. Chem. Research
Volume 35 (2) 2018 Pages No. 785-806

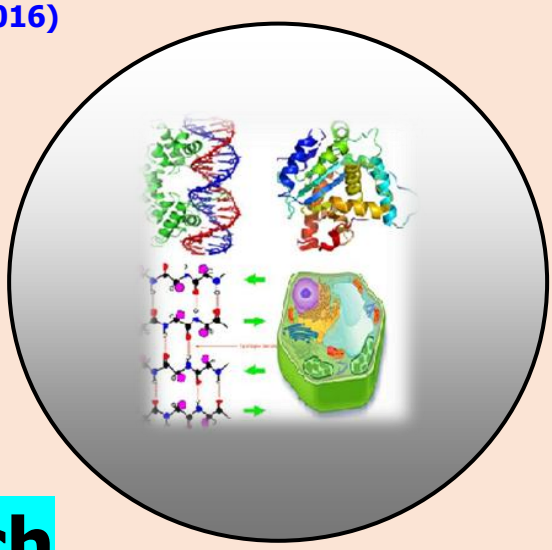

Journal of Biological and Chemical Research

An International Peer Reviewed / Referred Journal of Life Sciences and Chemistry

Indexed, Abstracted and Cited in various International and National Scientific Databases

Published by Society for Advancement of Sciences®

J. Biol. Chem. Research. Vol. 35, No. 2: 785-806, 2018
(An International Peer Reviewed / Refereed Journal of Life Sciences and Chemistry)
Ms 35/02/1204/2018
All rights reserved
ISSN 2319-3077 (Online/Electronic)
ISSN 0970-4973 (Print)

http:// www.sasjournals.com
http:// www.jbcr.co.in
jbiolchemres@gmail.com

RESEARCH PAPER

Received: 14/09/2018 **Revised: 05/10/2018** **Accepted: 06/10/2018**

Spectral analysis, DFT calculations on molecular structure, NBO, NLO and thermodynamic properties, multiple interactions and AIM approach of 4-(4-nitrophenyl)-2-oxo-7-phenyl-2,3,4,5,6,7-hexahydro-1H-pyrrolo[2,3-d]pyrimidine-5-carboxylic acid

Huda Parveen, Abha Bishnoi, *Shaheen Fatma and Poornima Devi

Department of Chemistry, University of Lucknow, Lucknow 226007, India
***Department of Chemistry, Shri Ramswaroop Memorial University, Dewa Road, Barabanki 225003, India**

ABSTRACT

The structure of newly synthesized biginelli product 4-(4-nitrophenyl)-2-oxo-7-phenyl-2,3,4,5,6,7-hexahydro-1H-pyrrolo[2,3-d]pyrimidine-5-carboxylic acid (4) of 5-oxo-1-phenylpyrrolidine-3-carboxylic acid has been confirmed with the help of various spectral techniques like UV, FT-IR, ^{1}H, ^{13}C NMR and mass spectroscopy. All quantum chemical calculations such as polarizability, hyperpolarizabilities, NBO, NLO, heat capacity, entropy and enthalpy change have been carried out at level of density functional theory (DFT) with B3LYP function using 6-31G(d,p) basis atomic set. The value of total first static hyperpolarizability (β_{tot}) has been found to be 20.5468×10^{-30} esu, indicating that the title molecule could be an attractive future NLO material. All the possible transitions have been computed by NBO analysis and correlated with the electronic transitions. MESP plot has been derived and electrophilic and nucleophilic regions have been identified with the help of this plot. HOMO and LUMO energy values and the difference between the two has been calculated along with the computation of electronegativity and electrophilicity indices.

Keywords: Natural Bond Orbital (NBO), thermodynamic properties, non linear optical (NLO), molecular electrostatic potential (MESP) and atom in molecule (AIM).

INTRODUCTION

As per literature, most of the compounds containing heterocyclic moiety are very active against several microorganism, and synthesis of such compounds have been dragging the eyes of chemist from a long time (John et al. 2004). Many heterocyclic compounds with pyrrolidine ring system, have been reported to exhibit an outstanding range of biological activities and the replacement of hydrogens of afore mentioned ring system by diversified substituents may lead to the various type of fruitful pharmacologically active compounds (Alan et al. 2003). A vast range of pharmacological activities such as anticonvulsant (Jolanta et al. 2003, Barbara 2005), antimicrobial (Lokhande et al. 2003, Mary et al. 2006, Donas et al. 2006), anti- HIV-1 (Shinichi et al. 2004**)** and antitumor (Xun et al. 2006) have been reported for compounds bearing pyrrolidine moiety in their skeletal

structure. Pyrrolidine derivatives also play an important role as inhibitors like ketoamide-based cathepsin K inhibitors (Barrett et al. 2006), human melanocortin-4 receptor agonists (Tran et al. 2007) and malic enzyme inhibitors (John et al. 2006). In this paper, the structure of synthesized compound 4 has been illustrated through different type of spectroscopic methods and a complete comparison has been made between the experimental and calculated data (obtained through DFT) of the compound 4. For DFT studies, it is important to choose a basis set which is well able to approximate the actual wave functions to provide chemically meaningful results. The shape of atomic orbitals gets distorted in molecule formation (polarization) and orbitals are influenced by other nuclei. To describe molecules with lone pairs, anions, transition states and excited states (loosely held e^-) diffuse basis sets can be useful, therefore the DFT calculation results including mulliken atomic charges, mesp, nlo, electronic absorption spectra, nbo, thermodynamic properties, local reactivity descriptors and global reactivity descriptors have been drawn using density functional theory (DFT) method with B3LYP function using 6-31g (d,p) basis atomic set. Distribution of density of electrons in various bonding and anti-bonding orbitals have been elicited by NBO analysis.

MATERIALS AND METHOD

NMR spectra of the compound 4 have been recorded on a Bruker 300 MHz instrument using TMS as internal reference and DMSO-d_6 as a solvent. Abbreviations for singlet, doublet, triplet and multiplet are quoted as s, d, t and m respectively. KBr pellet has been used for recording IR spectrum on a Perkin-Elmer Fourier transform infra-red spectrophotometer. DMSO has been used as a solvent for obtaining Ultraviolet spectrum, in the region 200-500 nm on UV-visible Double-Beam Spectrophotometer (systronic-2203) instrument. The HRMS of compound 4 has been recorded on a TOF MS ES- mass spectrometer. Thin-layer chromatography (TLCs) and an iodine chamber (to develop TLCs) have been used to check the progress of reaction. Synthesis of 5-oxo-1-phenylpyrrolidine-3-carboxylic acid (1) has been done by the reported method (Paytash et al. 1950).

Procedure for synthesis of 4-(4-nitrophenyl)-2-oxo-7-phenyl-2, 3, 4, 5, 6, 7-hexahydro-1H-pyrrolo [2,3-d] pyrimidine-5-carboxylic acid (4)

A mixture of 5-oxo-1-phenylpyrrolidine-3-carboxylic acid (1) (0.005 mol), 4-nitrobenzaldehyde (2) (0.005 mol), urea (3) (0.005 mol) and ethanol (15 mL) was refluxed under strong acidic condition (conc. HCl) for ~19 hrs at 100-110 0C. The reaction mixture was concentrated and kept overnight. Yellowish low melting solid was separated. The resulting yellowish oily product was purified by column chromatography using ethyl acetate-hexane (9.5:0.5 v/v). (Scheme 1) Yield: 41; Rf value: 0.43 [Hexane: Ethyl acetate] (8.0:2.0 v/v) as mobile phase; IR (KBr) ν_{max}. 2850 (=CH stretching); 2981.95 (-CH stretching), 1730.15 (C=O stretching); 3360 (-NH stretching); 3480 (-OH stretching); 1307.74(-C-N stretching); 1128.36(-C-O stretching), ^{1}H NMR (DMSO-d_6): δ (ppm) = 6.20-8.3 (m, 9H, phenyl ring), 2.5-2.8 (d, 2H, CH2 in pyrrolidine ring), 3.9-4.1 (m, 1H in pyrrolidine), 5.816 (s, 2H, NH), 5.44 (s, 1H in pyrimidone ring), 11(hydroxyl proton of carboxylic acid), ^{13}C NMR (DMSO-d_6): δ=59.19, 50.23, 119.86, 123-129, 139.47, 172.04, 150.74, 158-156; m/z: 380.3540.

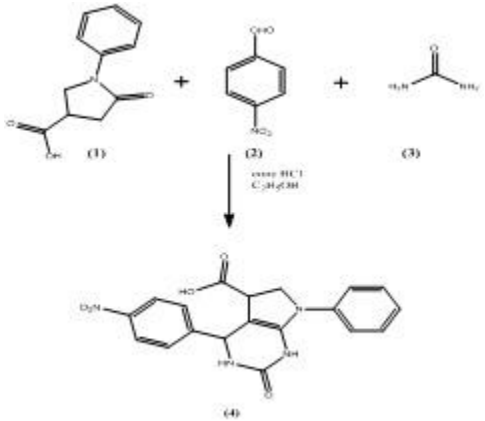

Scheme 1. Synthesis of 4-(4-nitrophenyl)-2-oxo-7-phenyl-2,3,4,5,6,7-hexahydro-1H-pyrrolo[2,3-d] pyrimidine-5-carboxylic acid (compound 4).

Computational Details

The quantum chemical results of compound 4 for theoretical and experimental consistency, have been obtained by DFT with B3LYP/6-31G(d,p) (Becke 1993, Becke 1988, Lee 1988), 6-31G(d,p) basis set has been used due to the polarization of atomic orbitals during the formation of molecular orbitals with Gaussian 09 package (Schlegel 1982). Calculated IR and UV spectra of compound 4 have been plotted by using GaussView05 program. Gauge Induced atomic orbital (GIAO) method has been implemented for getting NMR chemical shifts of the compound 4 (Wolinski et al. 1990). The Frontier orbital values have been obtained by imposing time dependent density functional theory (TD-DFT) at B3LYP/6-31-G(d,p) level with the implementation of IEFPCM model and DMSO as a solvent (Cossi et al. 2001, Adamo et al.2000). Intramolecular interactions, ring critical points, bond critical paths, ring critical point to bond critical paths and ring critical point attractor path have been obtained by AIM approach (Bader et al. 2000).

RESULTS AND DISCUSSION

Molecular geometry

Calculated optimized parameters like bond lengths, bond angles and dihedral angles of compound 4 have been compared with the experimental one (Table 1). All the essential experimental structural parameters have been taken from the similar systems for which the crystal structures have been solved. Figure 1 shows all the atoms present in the compound 4.

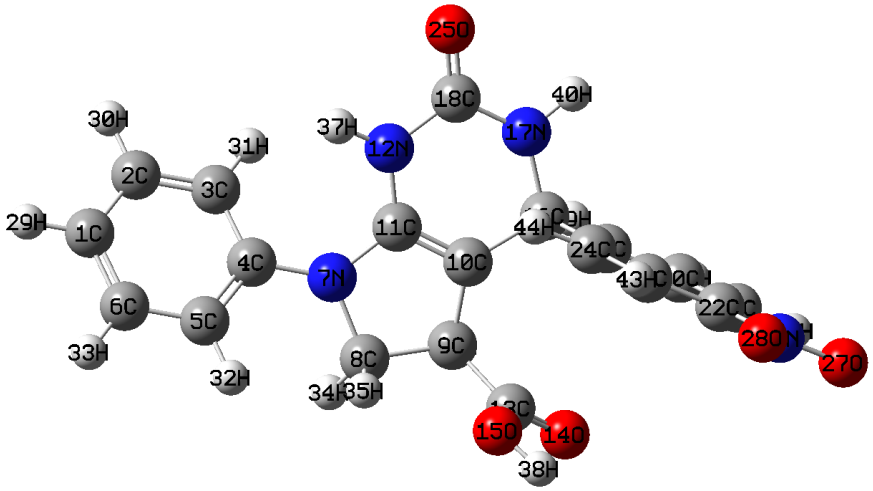

Figure 1. Optimized structure of compound 4.

The pure single bond character has been confirmed by comparing the calculated distance between C8-C9 (1.5541) with experimental distance between C8-C9 (1.525). The shortest bond of the compound 4 is O15-H38 (0.9723Å). All C-C bond length and C-H bond length of rings are in the range of 1.3-1.6 Å and 1.08-1.1 Å respectively. The variations observed in the bond angles are due to the electro negativity of the central atom, lone pair of electrons and the conjugation of the double bonds.

^{1}H and ^{13}C NMR spectra

^{1}H and ^{13}C NMR spectra (experimental and theoretical) of compound 4 has been presented in Table 2. The correlation graphs of experimental and calculated ^{1}H and ^{13}C NMR spectra have been shown in Fig. 2(a) & 2(b) respectively. The linear equations followed by correlation graphs are y = 1.018x - 0.853 for ^{1}H NMR and y = 0.950 x + 0.298 for ^{13}C NMR. Where 'y' and 'x' are the experimental and the calculated chemical shifts respectively. Solvent used for recording the NMR spectra was DMSO-d_6. Good agreement between the obtained experimental values and calculated values has been visualized from the correlation values (R^2 = 0.996 using B3LYP for ^{1}H NMR and R^2 = 0.991 using B3LYP for ^{13}C NMR).

Table 1. Comparison of calculated and experimental optimized structural parameters for title compound 4 using B3LYP/6-31G (d,p) method.

Bond Length	B3LYP	Exp	Bond Length	B3LYP	Exp
C1-C2	1.3957	1.381	N12-C18	1.3972	
C1-C6	1.3952	1.375	N12-H37	1.0089	
C1-H29	1.0852	0.93	C13-O14	1.211	
C2-C3	1.3934	1.3927	C13-O15	1.3538	
C2-H30	1.086	0.93	O15-H38	0.9723	
C3-C4	1.4083	1.396	C16-N17	1.4733	
C3-H31	1.0846	0.93	C16-C19	1.5349	
C4-C5	1.4053	1.382	C16-H39	1.103	
C4-N7	1.407	1.42	N17-C18	1.3738	
C5-C6	1.3938	1.38	N17-40H	1.0102	
C5-H32	1.0843	0.93	C18-O25	1.221	
C6-H33	1.0861	0.93	C19-C20	1.3986	1.39
N7-C8	1.4737	1.472	C19-C24	1.4028	1.39
N7-C11	1.3921		C20-C21	1.394	1.38
C8-C9	1.5541	1.525	C20-H41	1.0861	0.93
C8-H34	1.0924	0.97	C21-C22	1.3914	1.39
C8-H35	1.0963	0.97	C21-42H	1.0826	0.93
C9-C10	1.5176		C22-C23	1.3962	1.39
C9-C13	1.5218	1.52	C22-N26	1.4714	
C9-H36	1.0993	0.98	C23-C24	1.389	1.38
C10-C11	1.3502		C23-43H	1.0826	0.93
C10-C16	1.5001		C24-44H	1.0854	0.93
C11-N12	1.3786		N26-O27	1.2309	
			N26-O28	1.2312	
Bond Angle	**B3LYP**	**Exp**	**Bond Angle**	**B3LYP**	**Exp**
C2-C1-C6	119.1376	118.3	C4-C7-C11	127.4621	120.4
C2-C1-H29	120.4291	120.8	C8-N7-C11	106.6369	120.4
C6-C1-H29	120.4283	120.8	N7-C8-C9	104.1758	103.5
C1-C2-C3	120.7001	121.5	N7-C8-H34	110.2139	111.1
C1-C2-H30	120.1368	119.2	N7-C8-H35	110.7667	111.1
C3-C2-H30	119.1433	119.2	C9-C8-H34	113.0581	111.1
C2-C3-C4	120.2638	119.9	C9-C8-H35	109.4356	111.1
C2-C3-H31	119.9076	120.1	H34-C8-H35	109.1245	109.0
C4-C3-H31	119.7738	120.1	C8-C9-C10	101.1705	104.4
C3-C4-C5	118.8114	118.4	C8-C9-C13	114.3564	113.0
C3-C4-N7	120.5778	119.1	C8-C9-H36	111.3374	108.1
C5-C4-N7	120.5534	119.1	C10-C9-C13	114.2753	
C4-C5-C6	120.255	120.9	C10-C9-H36	111.2028	108.1
C4-C5-H32	120.1067	119.5	C13-C9-H36	104.7253	108.1
C6-C5-H32	119.6356	119.5	C9-C10-C11	108.4019	
C1-C6-C5	120.7869	121.0	C9-C10-C16	128.252	
C1-C6-H33	120.056	119.5	C11-C10-C16	122.2402	
C5-C6-H33	119.1537	119.5	N7-C11-C10	113.3774	
C4-N7-C8	122.968	120.4	N7-C11-N12	123.1893	
C10-C11-N12	123.3828		C20-C21-H42	121.9179	
C11-N12-C18	120.9288		C22-C21-H42	119.6047	
C11-N12-H37	122.1877		C21-C22-C23	122.0167	

C18-N12-H37	115.9442		C21-C22-N26	119.0244	
C9-C13-O14	123.9551		C23-C22-N26	118.9586	
C9-C13-O15	113.3616		C22-C23-C24	118.6054	
O14-C13-O15	122.6588		C22-C23-H43	119.4429	
C13-O15-H38	106.1305		C24-C23-H43	121.9516	
C10-C16-N17	108.1627		C19-C24-C23	120.7911	
C10-C16-C19	113.7756		C19-C24-H44	119.4935	
C10-C16-H39	109.6727		C23-C24-H44	119.7153	
N17-C16-C19	110.4498		C22-N26-O27	117.7328	
N17-C16-H39	108.1053		C22-N26-O28	117.6491	
C19-C16-H39	106.5383		O27-N26-O28	124.618	
C16-N17-C18	129.29		C21-C22-C23	121.9179	
C16-N17-H40	117.424		C21-C22-N26	119.6047	
C18-N17-H40	112.2066		C23-C22-N26	122.0167	
N12-C18-N17	115.1507		C22-C23-C24	119.0244	
N12-C18-C25	121.373		C22-C23-H43	118.9586	
N17-C18-C25	123.4612		C24-C23-H43	118.6054	
C16-C19-C20	120.3192		C19-C24-C23	119.4429	
C16-C19-C24	120.4669		C19-C24-H44	121.9516	
C20-C19-C24	119.2139		C23-C24-H44	120.7911	
C19-C20-C21	120.8941		C22-N26-O27	119.4935	
C19-C20-H41	119.678		C22-N26-O28	119.7153	
C21-C20-H41	119.4253		O27-N26-O28	117.7328	
C20-C21-C22	118.4774				
Dihedral Angle	**B3LYP**		**Dihedral Angle**	**B3LYP**	
C6-C1-C2-C3	-0.015		C3-C4-C5-H32	179.4257	
C6-C1-C2-H30	178.3522		N7-C4-C5-C6	-178.4481	
H29-1-2-3	-179.2019		N7-C4-C5-H32	2.1642	
H29-1-2-H30	-0.8347		C3-C4-N7-C8	-154.7066	
C2-C1-C6-C5	1.2597		C3-C4-N7-C11	47.3301	
C2-C1-C6-H33	-179.427		C5-C4-N7-C8	22.5063	
H29-C1-C6-C5	-179.5534		C5-C4-N7-C11	-135.457	
H29-C1-C6-H33	-0.2402		C4-C5-C6-C1	-0.6487	
C1-C2-C3-C4	-1.8363		C4-C5-C6-H33	-179.9681	
C1-C2-C3-H31	175.466		H32-C5-C6-C1	178.7419	
H30-C2-C3-C4	179.7805		O14-C13-O15-H38	1.1034	
H30-C2-C3-H31	-2.9171		C10-C16-N17-C18	9.2232	
C2-C3-C4-C5	2.417		C10-C16-N17-H40	176.3101	
C2-C3-C4-N7	179.6778		C19-C16-N17-C18	-115.888	
H31-C3-C4-C5	-174.8889		C19-C16-N17-H40	51.1989	
H31-C3-C4-N7	2.3718		H39-C16-N17-C18	127.9096	
C3-C4-C5-C6	-1.1866		H39-C16-N17-H40	-65.0035	
C10-C16-C19-C20	117.5318		C19-C20-C21-H42	179.8584	
C10-C16-C19-C24	-62.4586		H41-C20-C21-C22	-179.6165	
N17-C16-C19-C20	-120.6107		H41-C20-C21-H42	0.4453	
N17-C16-C19-C24	59.3989		C20-C21-C22-C23	0.2544	
H39-C16-C19-C20	-3.4361		C20-C21-C22-N26	-179.9415	
H39-C16-C19-C24	176.5735		H42-C21-C22-C23	-179.806	
C16-N17-C18-N12	-11.2556		H42-C21-C22-N26	-0.0018	

C16-N17-C18-C25	170.1442		C21-C22-C23-C24	0.0175	
H40-N17-C18-N12	-178.884		C21-C22-C23-H43	179.9056	
H40-N17-C18-C25	2.5158		N26-C22-C23-C24	-179.7868	
C16-C19-C20-C21	179.8961		N26-C22-C23-H43	0.1013	
C16-C19-C20-H41	-0.6923		C21-C22-N26-O27	0.804	
C24-C19-C20-C21	-0.1133		C21-C22-N26-O28	-179.0842	
C24-C19-C20-H41	179.2983		C23-C22-N26-O27	-179.3858	
C16-C19-C24-C23	-179.6156		C23-C22-N26-O28	0.726	
C16-C19-C24-H44	0.5126		C22-C23-C24-C19	-0.3453	
C20-C19-C24-C23	0.3939		C22-C23-C24-H44	179.5262	
C20-C19-C24-H44	-179.478		H43-C23-C24-C19	179.7695	
C19-C20-C21-C22	-0.2035		H43-C23-C24-H44	-0.3589	

Table 2. Calculated and experimental ^{1}H NMR chemical shifts (δ /ppm) of compound 4.

	Chemical Shift (ppm)			Chemical Shift (ppm)	
Atoms	B3LYP	Experimental	Atoms	B3LYP	Experimental
C1	120.3151		H29	7.1816	
C2	127.5846		H30	7.5155	
C3	117.3746	123-129	H31	7.1441	6.20-7.6
C4	138.2737		H32	7.0534	
C5	115.8497		H33	7.5435	
C6	128.4763		H34	3.5816	2.5-2.8
C8	57.1497	59.19	H35	4.4082	
C9	52.2008	50.23	H36	3.7582	3.9-4.1
C10	83.2353	119.86	H37	5.8319	5.816
C11	138.0429	139.47	H40	5.545	
C13	169.6175	172.04	H39	5.3325	5.44
C18	144.3268	150.74	H41	7.3402	
C19	152.0906		H42	8.3382	7.6-8.3
C20	127.7145		H43	8.5028	
C21	122.5639	158-156	H44	7.9829	
C22	146.9672				
C23	123.5591				
C24	129.0135				

Electronic absorption

The UV-Visible spectrum of compound 4 has been studied by TD-DFT method using the previously mentioned DFT method in section 3. The percentage contribution of probable transitions, corresponding absorption wavelengths along with simulated UV data, oscillator strength (f) and vertical excitation energies have been texted in Table 2 and compared with experimental results. An intense electronic transition at 311.03 nm with an oscillator strength ƒ = 0.1481 in DMSO has been anticipated which has been found to be very close to the experimental (λexp. = 318 nm in DMSO). Figure 3 shows the experimental and calculated spectra of compound 4, and the corresponding transitions from HOMO to LUMO+2 with 44.17% , HOMO-2 to LUMO with 33% and HOMO-5 to LUMO with 17.18% contribution have been texted in the table 3 and shown in the figure 4. These transitions happened due to n→π* and π →π*transition.

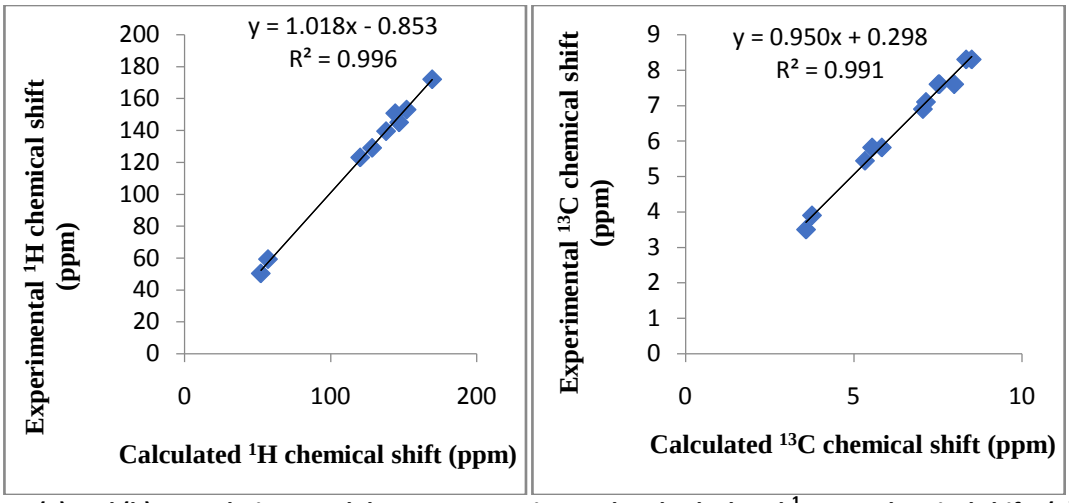

Figure 2 (a) and (b). Correlation graph between experimental and calculated ^{1}HNMR chemical shifts (a) and between experimental and calculated ^{13}CNMR chemical shifts (b) using B3LYP 6-31G (d, p).

Table 3. Experimental and theoretical absorption wavelength λ_{max} (nm), excitation energies E (eV) of compound 4 using B3LYP functional and 631-G/(d,p) basis set.

S. No	Electronic transitions (Molecular orbital involved)	Energy (in eV)	Calculated λ_{max} (in nm) B3LYP	Oscillatory strength (ƒ)	Percentage contribution of probable transition B3LYP	Observed λ_{max} (in nm)
1	97→100 (H-2→L)	3.9264	315.77	0.1323	33.02%	
2	99→102 (H→L+2)	3.9863	311.03	0.1481	44.17%	318
3	94→100 (H-5→L)	4.4452	278.92	0.3284	17.18%	

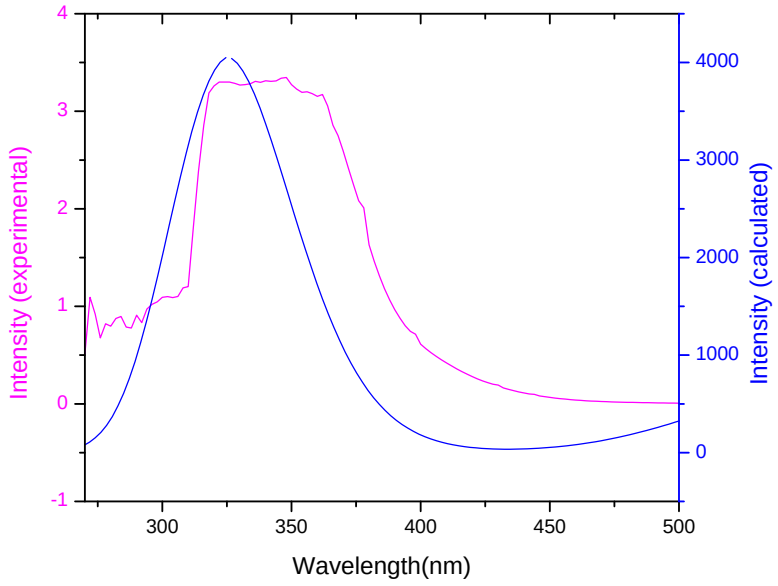

Figure 3. Experimental and theoretical UV-Visible spectra of compound 4.

Indexed, Abstracted and Cited in Indexed Copernicus International and 20 other databases of National and International repute

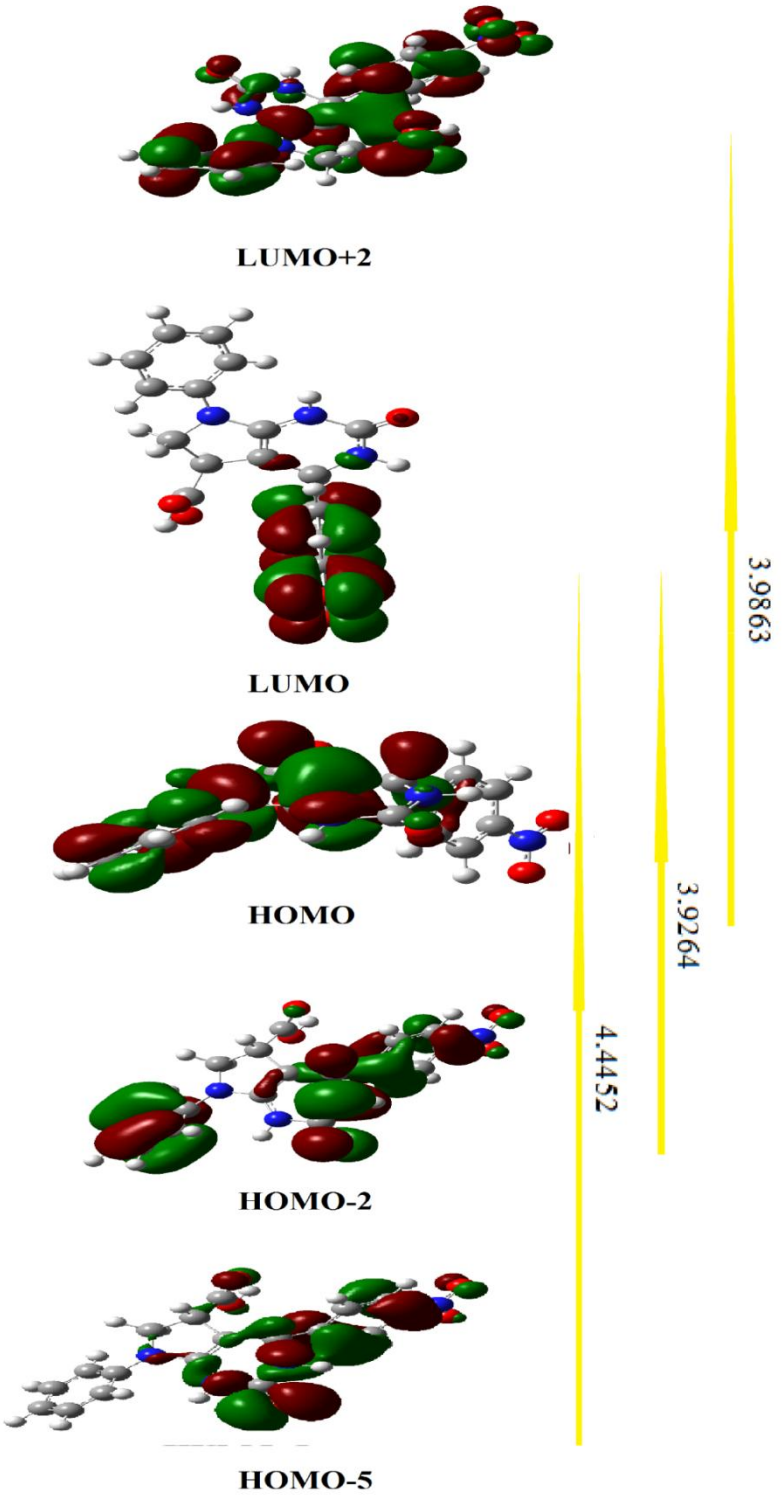

Figure 4. Transition between HOMO to LUMO+2, HOMO-2 to LUMO and HOMO-5 to LUMO.

Table 4. The potential energy distribution (PED) and, the calculated and experimental frequencies of the compound 4.

Theoretical wave numbers				
Unscaled	Scaled	Exp	I_{IR} (km/mol)	Vibrational Assignment (PED >10 %)
532.34	514.61		3.4	B (C21-N26-C22)(29.) β (C22-O28-N26)(16.) δ(C21-N26-C22-O28)(12.) -δ(25-12-18-37)(11.)
537.68	519.77		21.16	δ(25-12-18-37)(24.) δ (40-16-17-10)(21.) δ (H40-C16-N17-C10) (20.)
557.56	538.99		99.88	δ(H40-C16-N17-C10)(34.) δ(40-16-17-10)(23.) -π(40-16-18-17)(18.)
572.7	553.62		17.93	δ(40-16-17-10)(33.)
608.57	588.30		54.3	δ(36-13-9-14)(26.) -δ(12-10-11-9)(11.)
619.7	599.06		23.84	δ(40-16-17-10)(48.) δ(12-10-11-9)(14.) -β(17-25-18)(13.)
630.39	609.39		2.05	β(C1-C3-C2)(38.) -τ(10-11)(18.)
632.81	611.73		28.62	δ(40-16-17-10)(31.) -τ(10-11)(23.) δ(25-12-18-37)(13.)
640.72	619.38		2.55	β(C19-C21-C20)(33.) δ(40-16-17-10)(16.) -β(17-25-18)(14.) δ(25-12-18-37)(11.)
657.43	635.53		4.16	τ(10-11)(29.) δ(12-10-11-9)(28.) τ(N7-C8)(15.)
671.47	649.11		16.94	δ(25-12-18-37)(30.) -β(17-25-18)(17.)
691.33	668.30		3.17	τ(10-11)(23.) τ(N7-C8)(12.) β(C24-C20-C19)(12.)
712.01	688.30		8.21	π(C16-C20-C24-C19)(18.) -τ(C19-C20)(15.) δ(25-12-18-37)(12.)
715.57	691.74		17.52	τ(C1-C2)(42.) δ(40-16-17-10)(10.)
733.3	708.88		15.16	π(O25-N12-N17-C18)(39.) -δ(25-12-18-37)(22.) δ(25-12-18-37)(10.)
736	711.49		18.26	π(O25-N12-N17-C18)(55.) -δ(25-12-18-37)(32.)
767.17	741.62		8.53	π(C16-C20-C24-C19)(21.) -τ(C19-C20)(16.) π(C26-C21-C23-C22)(16.) -β(17-25-18)(13.)
768.65	743.05		48.33	π(O14-C9-O15-C13)(18.) -δ(40-16-17-10)(14.) -δ(12-10-11-9)(11.)
777.37	751.48		4.03	δ(25-12-18-37)(18.) π(O14-C9-O15-C13)(14.) -β(17-25-18)(11.)
818.73	791.46		66.32	ν(C16-C19)(11.)
834.87	807.06		7.17	δ(40-16-17-10)(18.) -δ(36-13-9-14)(18.) π(O14-C9-O15-C13)(17.)
847.99	819.75		2.11	π(H32-C4-C6-C5)(28.) -π(H31-C2-C4-C3)(16.) -π(H30-C1-C3-C2)(14.)
850.86	822.52		2.87	π(H44-C19-C23-C24)(38.) -π(H43-C22-C24-C23)(31.) π(H42-C20-C22-C21)(24.)
870.26	841.28		13.49	δ(25-12-18-37)(13.) -τ(C19-C20)(11.) δ(12-10-11-9)(10.)
874.44	845.32		24.69	τ(C19-C20)(25.) -π(C16-C20-C24-C19)(11.) -δ(12-10-11-9)(10.)
891.38	861.69		1.62	δ(25-12-18-37)(16.) -ν(N12-C18)(12.) δ(12-10-11-9)(12.)
910.31	879.99		4.76	π(H31-C2-C4-C3)(26.) π(H32-C4-C6-C5)(20.) -π(H29-C6-C2-C1)(20.)
923.04	892.30		10.95	δ(36-13-9-14)(30.) ν(N12-C18)(15.) δ(H36-C10-C9)(13.)
968.31	936.06		20.93	δ(40-16-17-10)(22.) - δ(H36-C8-C9)(20.) -δ(36-13-9-14)(18.) ν(N12-C18)(10.)
971.51	939.15		0.69	π(H33-C1-C5-C6)(34.) π(H30-C1-C3-C2)(21.) -π(H31-C2-C4-C3)(

				20.) π(H32-C4-C6-C5)(13.)
984.37	951.59		2.94	π(H42-C20-C22-C21)(43.) -π(H43-C22-C24-C23)(18.) -π(H44-C19-C23-C24)(17.) -τ(19-20)(11.)
987.44	954.55		2.19	π(H43-C22-C24-C23)(30.) π(H44-C19-C23-C24)(19.) π(H42-C20-C22-C21)(13.) τ(C19-C20)(13.)
995.28	962.13		0.59	π(H30-C1-C3-C2)(26.) -π(H29-C6-C2-C1)(23.) -π(H33-C1-C5-C6)(19.) -τ(C1-C2)(12.)
999.39	966.11		3.6	δ(H36-C8-C9)(34.) δ(40-16-17-10)(17.) δ(36-13-9-14)(16.)
1011.71	978.02		1.34	β(C6-C2-C1)(61.)
1031.97	997.60		6.1	β(C19-C21-C20)(54.)
1052.45	1017.40		12.32	δ(40-16-17-10)(18.) -δ(36-13-9-14)(18.)
1062.24	1026.86		10.28	δ(36-13-9-14)(23.) δ(36-13-9-14)(11.) δ(H36-C8-C9)(11.)
1092.54	1056.15		16.44	β(C69-H40-N17)(22.) -δ(40-16-17-10)(17.) β(17-25-18)(13.)
1105.2	1068.39		24.07	δ(40-16-17-10)(46.) -β(C69-H40-N17)(27.)
1122.55	1085.16	1037	3.83	δ(40-16-17-10)(19.) -ν(C10-C16)(12.)
1128.79	1091.20	1107	39.26	ν(C22-N26)(27.) -β(C19-C21-C20)(13.) -ν(C22-C23)(13.) -ν(C21-C22)(11.) β(C20-H42-C21)(10.)
1133.26	1095.52		1.95	δ(40-16-17-10)(40.) -β(C69-H40-N17)(17.)
1160.17	1121.53	1128	16.54	δ(25-12-18-37)(19.) -ν(N7-C8)(10.) ν(C11-N12)(10.) -ν(C9-C10)(10.)
1185.66	1146.17		118.93	δ(H36-C10-C9)(23.)
1189.16	1149.56		4.66	β(C6-H29-C1)(31.) -β(C1-H30-C2)(20.) β(C1-H33-C6)(17.)
1201.76	1161.74		13.43	δ(40-16-17-10)(27.)
1204.85	1164.72		12.68	δ(40-16-17-10)(15.) δ(H36-C8-C9)(12.)
1210.47	1170.16	1195	14.81	ν(C10-C16)(12.) β(C4-H32-C5)(11.) -β(C2-H31-C3)(10.) β(C1-H33-C6)(10.)
1212.57	1172.19	1226	10.48	δ(H36-C8-C9)(27.) ν(C10-C16)(14.) δ(36-13-9-14)(13.)
1286.05	1243.22		9.45	δ(H36-C8-C9)(32.) δ(H36-C13-C9-O14)(20.) - δ(H36-C10-C9)(13.)
1288.37	1245.46		76.66	δ(H36-C13-C9-O14)(40.) δ(H36-C8-C9)(28.) δ(H36-C10-C9)(12.)
1302.71	1259.32		67.45	δ(36-13-9-14)(32.) δ(H36-C10-C9)(19.)
1318.94	1275.01		5.75	δ(36-13-9-14)(44.) δ(H36-C10-C9)(42.) -δ(36-13-9-14)(10.)
1325.33	1281.19		0.46	δ(H36-C8-C9)(43.) δ(36-13-9-14)(29.)
1348.28	1303.38		2.58	δ(H36-C13-C9-O14)(41.) δ(H36-C8-C9)(32.)
1350.91	1305.92		38.39	δ(H36-C13-C9-O14)(23.) δ(H36-C10-C9)(18.)
1369.84	1324.22		3	δ(H40-C16-N17-C10)(14.) -β(C16-H40-N17)(13.) -β(C2-H31-C3)(12.)
1376.6	1330.75		57.84	δH(40-C16-N17-C10)(18.) -β(C69-H40-N17)(16.) -δ(H36-13-C9-O14)(11.)
1380.73	1334.75		262.43	δ(H36-C13-C9-O14)(43.) δ(H36-C8-C9)(18.) δ(H36-C10-C9)(16.)
1391.62	1345.27		89.06	δ(H40-C16-N17-C10)(29.) -β(C16-H40-N17)(18.)
1397.36	1350.82	1348	331.81	ν(N26-O27)(24.) ν(N26-O28)(24.) -ν(C22-N26)(14.)
1409.26	1362.33		16.66	β(C16-H40-N17)(38.) -δ(H40-C16-N17-C10)(37.)
1421.03	1373.70		125.16	β(C16-H40-N17)(28.) -δ(H40-C16-N17-C10)(23.) δ(O25-N12-C18-H37)(11.) -β(N17-O25-C18)(11.)

1463.3	1414.57		3.66	β(H39-N17-C16)(13.)
1472.54	1423.50		172.18	β(C16-H40-N17)(60.) -δ(H40-C16-N17-C10)(33.)
1496.36	1446.53	1500	11.98	β(C6-H29-C1)(16.) β(C16-H40-N17)(12.) -ν(C5-C6)(12.) ν(C2-C3)(12.)
1517.35	1466.8		53.66	ν(C2-C3)(45.)
1531.17	1480.18		5.15	β(C22-H43-C23)(18.) -β(C20-H42-C21)(15.) -ν(C22-C23)(12.) -ν(C21-C22)(11.)
1543.67	1492.26		55.1	β(C1-H30-C2)(11.) -β(C4-H32-C5)(10.) -ν(H34-H35-C8)(10.)
1550.89	1499.24		438.17	ν(C11-N12)(15.) -ν(N7-C11)(13.)
1617.94	1564.06		128.67	ν(N26-O27)(28.) -ν(N26-O28)(27.)
1632.77	1578.39		21.26	ν(C1-C6)(20.) -ν(C1-C2)(19.) -ν(C4-C5)(15.) ν(C3-C4)(13.)
1651.57	1596.57		41.31	ν(C23-C24)(23.) β(C24-C20-C19)(13.)
1658.46	1603.23		124.16	ν(C5-C6)(21.) ν(C2-C3)(21.) β(C6-C2-C1)(10.)
1670.34	1614.71		72.46	ν(N26-O27)(18.) -ν(N26-O28)(17.) -ν(C21-C22)(13.) β(C21-N26-C22)(13.) ν(C22-C23)(10.)
1734.95	1677.17		406.47	ν(C10-C11)(56.) δ(N12-C10-C11-C9)(18.)
1824.13	1763.38	1710	659.68	β(C16-H40-N17)(42.) -δ(H40-C16-N17-C10)(18.) -δ(O25-N12-C18-H37)(12.) -ν(C18-O25)(12.)
1839.18	1777.93	1730	240.23	δ(H36-C13-C9-O14)(44.) -ν(C13-O14)(32.) δ(H36-C10-C9)(11.)
2960.77	2862.17		55.47	ν(C16-H39)(98.)
3017.74	2917.24		29.36	ν(C9-H36)(96.)
3049.39	2947.84	2981	15.66	ν(C8-H35)(84.) ν(C8-H34)(14.)
3121.1	3017.16		18.41	ν(C8-H34)(83.) -ν(C8-H35)(14.)
3185.45	3079.37		5.73	ν(C6-H33)(41.) ν(C2-H30)(27.) -ν(C1-H29)(24.)
3192.31	3086.00		8.58	ν(C2-H30)(48.) -ν(C6-H33)(38.)
3194.36	3087.98		4.97	ν(C20-H41)(98.)
3203.75	3097.06		3.52	ν(C24-H44)(97.)
3207.5	3100.69	3100	22.7	ν(C1-H29)(50.) -ν(C3-H31)(32.) -ν(C5-H32)(13.)
3213.67	3106.65		12.43	ν(C3-H31)(46.) -ν(C5-H32)(34.) ν(C2-H30)(14.)
3217.51	3110.36		3.99	ν(C5-H32)(44.) ν(C1-H29)(20.) ν(C6-H33)(15.) ν(C3-H31)(10.)
3245.33	3137.26		1.19	ν(C23-H43)(97.)
3245.85	3137.76		1.38	ν(C21-H42)(97.)
3639.54	3518.34	3350	44.68	ν(N17-H40)(98.)
3654.83	3533.12	3460	105.09	ν(N12-H37)(95.)
3754.41	3629.38	3500	54.87	ν(O15-H38)(100.)

Vibrational Assignment

The vibrational data of novel 4-(4-nitrophenyl)-2-oxo-7-phenyl-2,3,4,5,6,7-hexahydro-1H-pyrrolo[2,3-d]pyrimidine-5-carboxylic acid (4) shows the presence of 44 atoms which belong to C1 point group possessing. One can look of the Figure 5 to compare the experimental and simulated vibrational spectra. The potential energy distribution (PED) and, the calculated and experimental frequencies of the compound 4 have been arranged in the supplementary Table 4.

OH vibrations

The reported range for has been found to be lie in the region 3600-3200 cm^{-1} (Colthup et al. 1990, Sathyanarayana 2004). In the experimental FT-IR spectrum, the OH stretching vibration has been observed at 3500cm^{-1} and found to be in good agreement with the calculated value at 3754$cm^{-1.}$

C–H vibration

In general most of IR frequency at 3085 cm^{-1} has been shown by hetero aromatic compounds due to asymmetric C-H stretching (Mekala et al.2016). The C-H stretching vibrations band of compound 4 have been observed at 2981 cm^{-1} and calculated band at 3185 cm^{-1}.

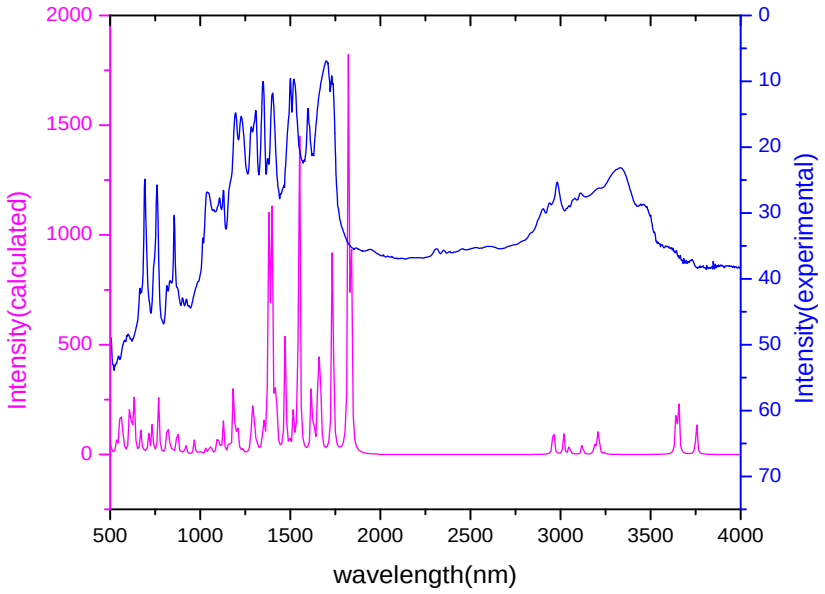

Figure 5. Experimental and calculated IR spectra of compound 4.

C-C vibrations

The C–C IR vibrations obtained through DFT method have been found at diverse values like 1031, 1052, 1122, 1128, 1201, 1348, 1531 and 1632 cm^{-1}as similar to the reported values at 1043, 1303,1443, 1470, 1533 and 1601cm^{-1} (Roja et al. 2011). However observed values of C-C stretching vibrations are at 1037, 1107, 1128, 1195, 1226, 1307, 1348, 1402 and 1500 cm^{-1} respectively. Hence the synthesis of compound 4 was confirmed both theoretically and experimentally.

C=O and C-O vibrations

The compound 4 possesses two carbonyl groups (C18=O25, C13=O14). The stretching vibrations of these carbonyl carbons have been observed at 1710 and 1730 cm^{-1} while the calculated vibrations of these carbonyl carbons have been found at 1824 and 1839 cm-$^{-1}$ in theoretical IR spectrum. The reported C=O stretching vibration is at 1703cm^{-1} (Harayama et al. 2004).

CH_2 vibrations

The FT-IR values of CH_2 vibrations, found at 2960, 3017, 3049, 3185 and 3192 cm^{-1} have shown similarity to the reported values appeared in the regions 3020-2855 cm^{-1} (Roeges 1994, Silverstein et al. 2003). On the other hand experimentally obtained FT-IR spectrum has shown values of CH_2 stretching vibrations between 2981- 3100 cm^{-1}.

NH vibrations

It has been found that the secondary amide group was present in compound 4. The stretching vibrations of both –NH– groups have been observed at 3350 and 3460 cm^{-1} while these values have been calculated at 3639 and 3654 cm^{-1}. The reported stretching vibration of –NH– in a secondary amide group has been found to be observed at 3500-3100 cm^{-1}.

Molecular electrostatic potential (MESP)

Hydrogen–bonding interactions, electron density and centre for electrophilic, and nucleophilic attacks have been explained through MESP plot (Prabavathi et al. 2014, Prasad et al. 2013). The molecular electrostatic potential contour surface of compound 4 has been visualized by the Figure 6. Different colors indicate the diverse values of the electrostatic potential at the surface in increasing order as follows (Grossman 2013, Singh et al. 2013, Zaater et al. 2016):

Red < yellow < green < light blue < blue

→→→→→→→→→→→→→→→→→

Figure 6 represented that the region around O25, O27 and O28 occupied more negative electrostatic potential with MEP value around -7.079 a.u than the region around C18, C22, C11, C13 and N26 with a MEP value of +7.079 a.u. From these values the following outputs have been obtained:

The most preferred regions for electrophilic attacks →O25, O27 and O28.

The most preferred regions for nucleophilic attacks → C22, C11, C13 and N26.

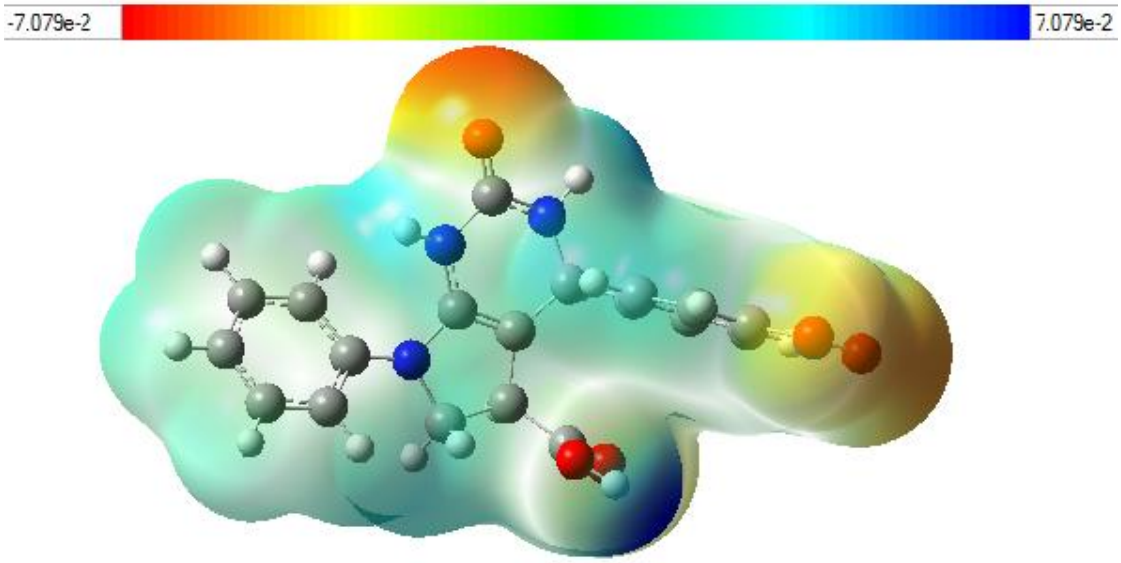

Figure 6. 3D plot of the molecular electrostatic potential of the compound 4.

Natural bond orbital analysis

The Gaussian09 package at the B3LYP/6-31 G (d,p) basis set has been put upon for NBO analysis (Glendening et al. 1998). Occupancy of donor and acceptor bonds, lone pair energy, hyper conjugative interactions in molecular systems, interactions between electron donors and electron acceptors and the stabilization energy values have been obtained from Natural bond orbital (NBO) analysis. It has been found that more intense interactions between electron donors and electron acceptors are those which possess larger stabilization energy value. The extent of conjugation is also proportional to stabilization energy value. The following equation (2) shows the correlation between stabilization energy E (2), occupancy of donor orbital (qi), diagonal elements of donor (i) and acceptor (j) level bonds (Ei and Ej respectively) and off diagonal NBO Fock matrix element (Fij) (Reed et al. 1988) in accordance with the second order Fock matrix in NBO analysis .

$$E(2) = \Delta E_{ij} = qi \frac{\left(F_{ij}\right)^2}{\left(E_j - E_i\right)} \quad (1)$$

The NBO analysis has been texted in Table 5. From this table it has been visualized that the some of the high energy charge transfers are from bonding π (C1-C6) to antibonding π* (C2-C3) and (C4-C5) and with stabilization energy of 22.85 and 19.39 kcal mol^{-1} respectively, presenting the presence of conjugated system,

and intramolecular charge transfers from π (C2-C3) to π* (C1-C6) and (C4-C5) with stabilization energy of 17.43 and 21.01 kcal mol^{-1} respectively. A charge transfer has also been noticed from π (C4-C5) to π*(C1-C6) with stabilization energy of 21.35 kcal mol^{-1}, showing aromatic character inside the system.

Few transitions such as from nonbonding orbital of O15 and N12 to π*(C13-O14) and (C10-C11) put forth very high stabilization energy of 47.18 and 40.75 kcal mol^{-1} respectively. In molecule 4 charge transfer from π of O14 to σ* (C13-C15) with stabilization energy of 34.5 kcal mol^{-1}, from nonbonding orbital of O25 to σ* orbitals of (N12-C18) and (N17-C18) with stabilization of 27.09 and 25.46 kcal mol^{-1} respectively and from nonbonding orbital of O27 to σ* orbital of (N26-N28) with stabilization of 19.27 kcal mol^{-1} have also been extracted from calculated data. All these charge transfers have been originated due to corresponding delocalization of electrons inside the system.

Table 5. Second order perturbation theory analysis of Fock matrix in NBO basis of the compound 4.

Donor	Type	occupancy(ED/e)	Acceptor	Type	Occupancy(ED/e)	E(2)*	Ej-Ei**	Fij***
C1-C6	π	1.66039	C2-C3	π*	0.33872	22.85	0.28	0.071
C1-C6	π	1.66039	C4-C5	π*	0.40303	19.39	0.27	0.066
C2-C3	π	1.69396	C1-C6	π*	0.33859	17.43	0.29	0.64
C2-C3	π	1.69396	C4-C5	π*	0.40303	21.01	0.28	0.07
C19-C20	π	1.63809	C21-C22	σ *	0.37042	23.31	0.28	0.072
C19-C20	π	1.63809	C23-C24	π*	0.2797	17.67	0.28	0.065
C4-C5	π	1.65452	C1-C6	π*	0.33859	21.35	0.29	0.071
C21-C22	σ	1.65331	C19-C20	π*	0.32581	16.95	0.3	0.064
C21-C22	σ	1.65331	C23-C24	π*	0.2797	19.82	0.3	0.07
C21-C22	n	1.65331	N26-O27	σ *	0.62708	24.7	0.15	0.058
C23-C24	σ	1.65684	C19-C20	σ *	0.32581	21.06	0.29	0.07
C23-C24	σ	1.65684	C21-C22	σ *	0.37042	19.99	0.28	0.067
N26-O27	n	1.98607	N26-O27	π*	0.62708	7.46	0.32	0.052
N7	n	1.71336	C4-C5	π*	0.40303	24.13	0.28	0.76
N7	n	1.71336	C10-C11	π*	0.30467	39.79	0.3	0.099
N12	n	1.71519	C10-C11	π*	0.30467	40.75	0.31	0.101
N12	n	1.71519	C18-O25	π*	0.32572	37.17	0.35	0.104
O14	n	1.84823	C9-C13	σ *	0.07137	19.2	0.63	0.101
O14	π	1.84823	C13-C15	σ *	0.10369	34.5	0.61	0.131
O15	n	1.81681	C13-O14	π*	0.20932	47.18	0.34	0.115
N7	n	1.71336	C18-O25	π*	0.32572	41.9	0.34	0.109
O25	n	1.84232	N12-C18	σ *	0.08331	27.09	0.65	0.121
O25	n	1.84232	N17-C18	σ *	0.07569	25.46	0.69	0.121
O27	n	1.8982	C22-N26	σ *	0.10406	12.59	0.57	0.076
O27	n	1.8982	N26-N28	σ *	0.05681	19.27	0.71	0.105
O28	n	1.89863	C22-N26	σ *	0.10406	12.53	0.57	0.075
O28	n	1.89863	N26-O27	π*	0.05663	19.23	0.71	0.105

Non -linear optical analysis

NLO shell outs major advantages (as well as some limitations) to some very important applications in sensors, commercial lasers, environmental monitoring, telecommunications, manufacturing, medicine and materials processing, in scientific and the military. NLO has generated high-resolution spectroscopy, enforced micromachining, offered new materials analysis tools, and high-capacity telecommunications. The high quality fiber optics systems that have been used to empower the internet, the technology used in advanced medical devices, in controlling water and air pollution, and in characterization of new materials have been offered by NLO (Elsa 2013). Organic aromatic systems possess polarization due to presence of conjugated π-bonds and the donor and acceptor groups which give rise to a high nonlinear optical coefficient. The following equations (2-4) have been applied to calculate the first hyperpolarizability β_{tot}, average polarizability α_{tot} and total dipole moment μ of the studied compound (4) employing the x,y,z components (Kleinman 1962).

$$\mu_{tot} = \left(\mu_x^2 + \mu_y^2 + \mu_z^2\right)^{1/2} \quad (2)$$

$$\alpha_{tot} = \frac{1}{3}\left(\alpha_{xx} + \alpha_{yy} + \alpha_{zz}\right) \quad (3)$$

$$\langle\beta\rangle = \left[\left(\beta_{xxx} + \beta_{xyy} + \beta_{xzz}\right)^2 + \left(\beta_{yyy} + \beta_{yzz} + \beta_{yxx}\right)^2 + \left(\beta_{zzz} + \beta_{zxx} + \beta_{zyy}\right)^2\right]^{1/2} \quad (4)$$

The corresponding data of electronic dipole moment μ (i = x, y, z), first hyperpolarizability and polarizability have been texted in Table 6. The calculated dipole moment, polarizability α_{tot} and first hyper polarizability for the title compound 4 are equal to 5.93 D, 0.9063×10^{-24}esu and 20.5468 ×10^{-30}esu respectively for B3LYP level.

Table 6. Dipole moment (μ_{tot}), polarizability (α_{tot}), anisotropy of polarizability (Δα) and static hyperpolarizability (β_{tot}) calculated at DFT/B3LYP/6-31G (d,p) level of theory.

Dipole Moment		Static Hyperpolarizability	
μ_x	-5.3864	β_{xxx}	1903.14
μ_y	-2.2788	β_{xxy}	140.02
μ_z	-0.9788	β_{xyy}	256.784
μ_{tot}	5.93	β_{yyy}	-177.734
		β_{xxz}	1013.48
Polarizability		β_{xyz}	-102.048
α_{xx}	-363.062	β_{yyz}	-54.29
α_{xy}	-28.0323	β_{xzz}	21.7555
α_{yy}	191.059	β_{yzz}	-62.6505
α_{xz}	-32.8524	β_{zzz}	-17.6555
α_{yz}	-789866	β_{tot}	20.5468×10^{-30}
α_{zz}	190.35	Δα	1107.386×10^{-30}
α_{tot}	0.906342×10^{-24}		

Thermo dynamical analysis

Thermo dynamical properties play momentous role in the accompaniment of numerous chemical and physical phenomena. In the present study, the DFT-B3LYP/6-31G(d,p) method has been applied to extort rotational constants and zero point vibrational energy at standard temperature (298.15 K) along with two statistical thermodynamic functions, entropy (S) and heat capacity (CV) at different temperatures (from 100 to 500 K), texted in the table 7(a) & 7(b) for the title compound 4.

The correlative graph of these thermodynamic properties and temperatures (T) has been shown in Figure 7. As the temperature increases from 100 to 500 K, the molecular vibrational intensities also increases that leads to the enhancement of heat capacity and entropy with the temperature. The fitting factors (R^2) for the heat capacity, entropy and temperatures have been found to be 0.998 and 0.99 respectively and can be used to find out other thermodynamic energies (gibbs free energy) and to estimate the feasibility of chemical reactions. All thermodynamic calculations have been performed in gas phase.

Table 7(a). Calculated thermodynamic parameters of compound 4 at standard temperature 298.15 K.

Parameters	B3LYP6-31G(d,p)
Zero point vibrational energy (Kcal/mol)	211.32576
Rotational temperature(K)	0.01669
	0.00447
	0.00411
Rotational constant(GHZ)	
X	0.34769
Y	0.09316
Z	0.08572
Total energy E_{total} (Kcal/mol)	225.990
Translational	0.889
Rotational	0.889
Vibrational	224.213

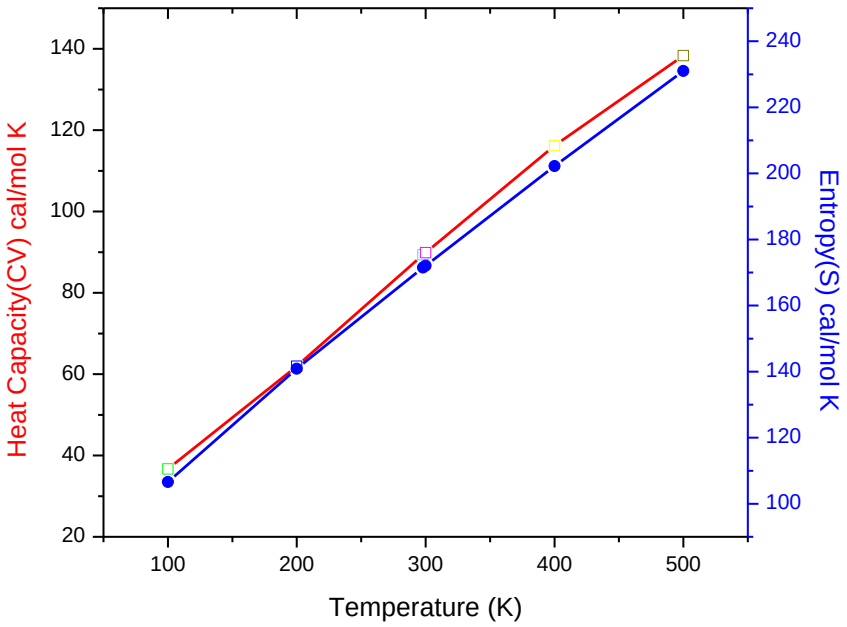

Figure 7. Correlation graph of heat capacity and entropy calculated at diverse temperature.

Table 7(b). Thermodynamic functions of compound 4 at different temperatures.

Temperature[K]	Heat capacity(CV) [Cal/molK](B3LYP)	Entropy(S) [Cal/molK](B3LYP)
100	36.683	106.588
200	61.936	140.889
298	89.376	171.509
300	89.891	172.076
400	116.204	202.193
500	138.356	231.031

Reactivity descriptors

Global Reactivity Descriptors

The computation of reactivity descriptors such as electronegativity (χ), global hardness (η), chemical potential (μ), electrophilicity index (ω) and global softness (S) have put forth an appreciable approach to predict global reactivity trends. In molecular systems, Koopman's theorem has been fundamentally imposed to ascertain site selectivity and chemical reactivity (Prasad et al. 2013, Arivazhagan et al. 2015, Soliman et al. 2015, Sethi et al. 2015).The afore mentioned reactivity descriptors have been calculated using following equations. [(5)-(12)] and texted in Table 8.

$$\mathrm{IP} = -\varepsilon_{HOMO} \quad (5)$$

$$\mathrm{EA} = -\varepsilon_{LUMO} \quad (6)$$

$$\chi = -\frac{1}{2}\left(\varepsilon_{LUMO} + \varepsilon_{HOMO}\right) \quad (7)$$

$$\mu = -\frac{1}{2}\left(I + A\right) \quad (8)$$

$$\eta = \frac{1}{2}\left(I - A\right) \quad (9)$$

$$\omega = \frac{\mu^2}{2\eta} \quad (10)$$

$$S = \tfrac{1}{2}\eta \quad (11)$$

$$\Delta N = -\mu / \eta \quad (12)$$

Table 8. Calculated frontier molecular orbitals (ƐLUMO, ƐHOMO), band gap (ƐLUMO-ƐHOMO), ionization potential (IP), electron affinity (EA), electronegativity (χ), global hardness(η), chemical potential (μ), global electrophilicity index (ω), global softness (S) and additional electronic charge (ΔN_{max}) of product 4 using B3LYP/6-31G(d,p) basis set.

	ε_H	ε_L	$\varepsilon_H - \varepsilon_L$	IP	EA	χ	η	μ	ω	S	ΔN_{max}
P	-0.1877	-0.09563	-0.0921	0.1877	0.0956	0.1416	0.0460	-0.1417	0.2181	10.86	3.0784

Local reactivity descriptors

Condensed Fukui Function (f_k) is a descriptor of the reactivity of an atom in a molecule. The condensed value around each atomic site indicates the atomic contribution of molecule. The f_k values are defined as

$$f_K^+ = \left[q(N+1) - q(N) \right] \text{for nucleophilic attack} \quad (13)$$

$$f_K^- = \left[q(N) - q(N-1) \right] \text{ for electrophilic attack} \quad (14)$$

$$f_K^0 = \frac{1}{2}\left[q(N+1) - q(N-1) \right] \text{ for radical attack} \quad (15)$$

Where, N, N–1, N+1 represent total electrons those are present in neutral, anionic and cationic states of molecule respectively.

The following equations define the local reactivity descriptors for site k

$$s_K^+ = Sf_K^+,\ s_k^- = Sf_K^-,\ s_K^0 = Sf_K^0 \quad (16)$$

$$\omega_K^+ = \omega f_K^+,\ \omega_K^- = \omega f_K^-,\ \omega_K^0 = \omega f_K^0 \quad (17)$$

Where +, –, 0 signs show attack of nucleophile, electrophile and radical respectively. The more prone site for nucleophilic or electrophilic attack than other atomic sites can be obtained through visualizing the values of all these local reactivity descriptors, higher vaues of these local reactivity descriptors indicate that these sites are liable to nucleophilic or electrophilic attack. Fukui functions (fk^+, fk^-), local electrophilicity indices (ωk^+, ωk^-) and local softnesses (sk^+, sk^-) (Parr et al. 1999, Chattaraj et al. 2007) for selected atomic sites of molecule have been texted in Table 9. The comparatively hiked values of local reactivity descriptors (fk^+, sk^+, ωk^+) observed at N26, C10, C5, C1 and C3 show that these sites are more liable to nucleophilic attack, where as the relatively high values of these descriptors (fk^-, sk^-, ωk^-) at C22, O27, O28, O25 and C24 suggest that these site are more prone for attack of electrophiles. These explorations have furnished enough information about the molecule for further studies.

Table 9. Hirshfeld population analysis: Fukui functions (fk^+, fk^-), local softnesses (sk^+, sk^-) in eV, local electrophilicity indices (ωk^+, ωk^-) in eV for selected atomic sites of compound 4.

	Hirshfield Atomic Charges			Fukui Functions		Local Softness		Local Electrophilicity Indices	
	q_N	q_N+1	q_N-1	f_k+	f_k-	sk^+	sk^-	ωk+	ωk^-
C1	-0.01731	0.091437	-0.03174	0.108746	0.014426	0.028033	0.003719	0.398086	0.052809
C2	-0.01378	0.059563	-0.01935	0.073347	0.005568	0.018907	0.001435	0.268501	0.020383
C3	-0.08264	0.014899	-0.04238	0.097538	-0.04026	0.025143	-0.01038	0.357057	-0.14739
C4	0.400842	0.271589	0.284005	-0.12925	0.116837	-0.03332	0.030118	-0.47316	0.427705
C5	-0.07935	0.032829	-0.03409	0.112175	-0.04526	0.028916	-0.01167	0.410639	-0.16566
C6	0.000093	0.055901	-0.02718	0.055808	0.027276	0.014386	0.007031	0.204296	0.099849
N7	-0.62564	-0.55639	-0.61358	0.06925	-0.01206	0.017851	-0.00311	0.253503	-0.04416
C8	0.242248	0.323682	0.214427	0.081434	0.027821	0.020992	0.007172	0.298105	0.101844
C9	-0.06738	-0.03531	-0.09728	0.032062	0.029902	0.008265	0.007708	0.117369	0.109462
C10	-0.03024	0.085583	0.027038	0.115826	-0.05728	0.029858	-0.01477	0.424004	-0.20969
C11	0.62266	0.620242	0.553564	-0.00242	0.069096	-0.00062	0.017812	-0.00885	0.25294
N12	-0.37252	-0.34646	-0.41314	0.026059	0.040627	0.006717	0.010473	0.095394	0.148723
C13	0.581551	0.600433	0.587585	0.018882	-0.00603	0.004867	-0.00156	0.069121	-0.02209
O14	-0.46144	-0.42557	-0.48067	0.035866	0.019236	0.009246	0.004959	0.131295	0.070417
C15	-0.15711	-0.12711	-0.16064	0.030006	0.003526	0.007735	0.000909	0.109843	0.012908
C16	0.143243	0.14913	0.07237	0.005887	0.070873	0.001518	0.01827	0.021551	0.259445
N17	-0.30551	-0.25856	-0.29759	0.046954	-0.00792	0.012104	-0.00204	0.171885	-0.02901
C18	0.681529	0.754948	0.724862	0.073419	-0.04333	0.018926	-0.01117	0.268765	-0.15863
C19	0.058574	0.124732	0.101131	0.066158	-0.04256	0.017054	-0.01097	0.242185	-0.15579
C20	-0.00205	-0.00804	-0.10304	-0.00599	0.100984	-0.00154	0.026032	-0.02191	0.369672
C21	0.070664	0.087086	-0.04132	0.016422	0.111981	0.004233	0.028866	0.060116	0.409929
C22	0.371298	0.247023	0.226802	-0.12428	0.144496	-0.03204	0.037248	-0.45493	0.528957

C23	0.011281	0.077967	-0.04227	0.066686	0.053549	0.01719	0.013804	0.244117	0.196027
C24	0.036118	-0.01755	-0.08471	-0.05367	0.120828	-0.01383	0.031147	-0.19646	0.442315
O25	-0.41939	-0.46561	-0.55085	-0.04622	0.131458	-0.01191	0.033887	-0.16918	0.481228
N26	0.222063	0.39014	0.330723	0.168077	-0.10866	0.043327	-0.02801	0.615279	-0.39777
O27	-0.40031	-0.3714	-0.54123	0.028914	0.140918	0.007453	0.036326	0.105845	0.515859
O28	-0.40749	-0.3752	-0.54146	0.032297	0.133968	0.008326	0.034534	0.11823	0.490417

AIM approach

In order to achieve diverse type of intramolecular interaction like strong, medium, weak H-bonds and their covalent, partially covalent and electrostatic nature, values of Laplacian of electron density {ρ(BCP)} and total electron density at bond critical point (H_{BCP}) should be known which can be obtained through implementation of AIM program to the compound 4 (Rozas et al. 2000). Figure 8 shows the molecular graph of compound 4 and, in table 10 parameters (geometrical and topological) for bonds of interacting atom have been texted.

Strong H-bonds $\nabla^2\rho(BCP) < 0$ and $H_{BCP} < 0$

Medium H-bonds $\nabla^2\rho\ (BCP) > 0$ and $H_{BCP} < 0$

Weak H-bonds $\nabla^2\rho(BCP) > 0$ and $H_{BCP} > 0$

As the (BCP) parameter and H_{BCP} parameter have been found to be greater than zero and less than zero respectively. Consequently N12-H37.....H31 is a medium interaction. From the AIM calculations it has been found that the total energy of intramolecular interactions is 0.511914 kcal/mol and the ellipticity value of this intramolecular hydrogen bond is +0.050208. The ε is related to λ1 and λ2, which corresponds to the eigen values of Hessian and connected by a relationship: ε = (λ1/ λ2) – 1. This value of ellipticity indicates the electron delocalization in the aromatic ring as ellipticity (ε) monitors the π-character of bond (Matta et al. 2007).

Table 10. Topological parameters for intramolecular interaction in compound 4 electron density (ρBCP), laplacian of electron density ($\nabla^2\rho$BCP), electron kinetic energy density (G_{BCP}), electron potential energy density (V_{BCP}), total electron energy density (H_{BCP}), hydrogen bond energy (E_{HB}) at bond critical point (BCP).

Interactions	ρ_{BCP}	$\nabla^2\rho_{BCP}$	G_{BCP}	V_{BCP}	H_{BCP}	E_{HB}
N12-H37.....H31	+0.34294	-1.84318	0.05111	-0.56303	-0.381553	0.511914
ρ_{BCP}, $\nabla^2\rho_{BCP}$, G_{BCP}, V_{BCP}, H_{BCP} in a.u. and E_{HB} in (kcal/mol)						

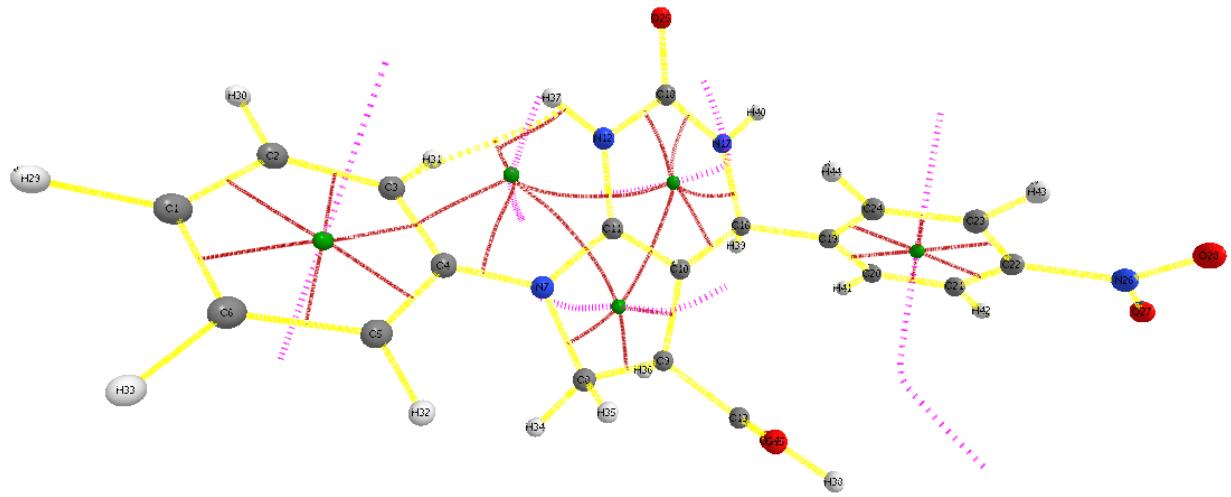

Figure 8. Molecular graph of the compound 4 using AIM program at B3LYP/6- 31G (d,p) level ring critical points (small green sphere), bond critical paths (yellow lines), ring critical point to bond critical paths (red lines) and ring critical point attractor path (purple lines).

CONCLUSION

The newly synthesized 4-(4-nitrophenyl)-2-oxo-7-phenyl-2,3,4,5,6,7-hexahydro-1H-pyrrolo[2,3-d]pyrimidine-5-carboxylic acid (4) has been characterized and quantum chemical calculations have been done with help of B3LYP/6-31G(d,p) basis set. Vibrational assignments of the wavenumbers have been carried out with the help of potential energy distribution approach. MESP technique has been used for assaying the centre of electrophillic and nucleophillic attacks, electron density, hydrogen–bonding interactions, structural and symmetry properties of compound 4. The confirmation of the hyper conjugative interactions and, inter and intra molecular interactions of the molecular system compound 4 have been analyzed by NBO analysis. The biological activity depends on the charge transfer, which is expected from calculated HOMO and LUMO energies, derived from second order perturbation theory. There was an excellent agreement with experimental data of chemical shift values as provided by GIAO NMR. The NLO analysis including hyperpolarizability, polarizability values and, total and partial dipole moment showed that the molecule is a claimant NLO material. The thermo dynamical analysis clearly indicated that the increase of the temperature led to increase in the thermo dynamical parameters like heat capacity and entropy. The results of the AIM approach (Ellipticity and intramolecular hydrogen bond interactions) depicted π-character of bonds in the aromatic ring and medium hydrogen bonds.

ACKNOWLEDGEMENTS

The authors convey their thanks to the Head, Department of Chemistry, Lucknow University, Lucknow, for providing laboratory facilities for spectral analysis and central facility for computational research and they are also thankful to the director of Kanpur IIT, Kanpur, for providing mass spectral data.

REFERENCES

Adamo, C. and Barone, V. (2000). A TDDFT study of the electronic spectrum of s-tetrazine in the gas-phase and in aqueous solution. *Chem. Phys. Lett*. 330 152–160.

Alan, R. K., Satheesh, K. N., Rachel, M. W. and Steven, M. H. (2003). Synthesis of 3, 3-diarylpyrrolidines from diaryl ketones. *Arkivoc* (V) 9-18.

Arivazhagan, M. and Kumar, J. S. (2015). Molecular structure, vibrational spectral assignments, HOMO–LUMO, MESP, Mulliken analysis and thermodynamic properties of 2, 6-xylenol and 2, 5-dimethyl cyclohexanol based on DFT calculation. *Spectrochimica Acta Part A: Molecular and Biomolecular Spectroscopy* 137 490–502**.**

Bader, R. F. W. and Cheeseman, J. R. (2000). *AIMPAC.*

Barbara, M. (2005). New anticonvulsant agents. *Current Topics in Medicinal Chemistry*. 5 69-85.

Barrett, D. G., Catalano, J. G., Deaton, D. N., Hassell, A. M., Long, S. T., Miller, A. B., Miller, L. R., Ray, J. A., Samano, V., Shewchuk, L. M., Wells-Knecht, K. J., Willard, D. H. Jr and Wright, L. L. (2006). Novel, potent P2-P3 pyrrolidine derivatives of ketoamide-based cathepsin K inhibitors. *Bioorg. Med. Chem. Lett.* 16 1735–1739.

Becke, A. D. (1988). Density-functional exchange-energy approximation with correct asymptotic behavior. *Phys. Rev. A* 38, 3098.

Becke, A. D. (1993). A new mixing of Hartree-Fock and local density functional theories. *J. Chem. Phys.* 98, 1372–1377.

Chattaraj, K. and Giri, S. (2007). Stability, Reactivity and Aromaticity of Compounds of a Multivalent Superatom. *J. Phys. Chem. A* 111, 11116–11121.

Colthup, N. B., Daly, L. H. and Wiberly, S. E. (1990). New York: *Academic Press*.

Cossi, M. and Barone, V. *J. (*2001). Time-dependent density functional theory for molecules in liquid solutions. *J. Chem. Phys.* 115, 4708–4717.

Donas, H. A., Yahya, N., Nizami, D. and Colin, K. (2006). Synthesis, Crystal Structure and Antifungal/Antibacterial Activity of Some Novel Highly Functionalized Benzoylaminocar bothioyl Pyrrolidines. *Turk J. Chem.* 30 573-583.

Elsa, G. (2013). Nonlinear optics in daily life. *OPTICS EXPRESS* 21 25. DOI:10.1364/OE.21.030532.

Glendening, E. D., Reed, A. E., Carpenter, J. E. and Weinhold, F. (1998). NBO Version 3.1, TCI, University of Wisconsin, Madison.

Grossman, M. D. (2013). *Procedia Computer Science* 18, 816 – 825.

Harayama, T., Hori, A., Serban, G., Morikami, Y., Matsumoto, T., Abe, H. and Takeuchi, Y. (2004). Concise synthesis of quinazoline alkaloids, luotonins A and B and rutaecarpine. *Tetrahedron* 60, 10645–10649.

John, H. B., John, M. B., Wilson and Gisvold (2004). *Textbook of Organic Medicinal and Pharmaceutical Chemistry* (ed.) (Philadelphia: Lippincott Williams and Wilkins) p.1.

John, Z. Y., Zhaolin, W., Dennis, S. and Roustem, N. (2006). In silico design and synthesis of piperazine-1-pyrrolidine-2,5-dione scaffold-based novel malic enzyme inhibitors. *Bioorg. Med. Chem. Lett.* 16 525-528.

Jolanta, O. and Agnieszka, Z. (2003). Synthesis and anticonvulsant properties of new N-[(4-phenyl phenylpiperazin-1-yl)-methyl] derivatives of 3-phenylpyrrolidine-2,5-dioneand 2-aza-spiro[4.4]nonane-1,3-dione. *Il Farmaco* 58 1227-1234.

Kleinman, D. A. (1962). Nonlinear Dielectric Polarization in Optical Media. *Phys. Rev*. 126 1977–1979.

Lee, C., Yang, W. and Parr, R. G. (1988). Development of the Colle-Salvetti correlation-energy formula into a functional of the electron density. *Phys. Rev. B Condens Matter* 37 785.

Lokhande, T. N., Bobade, A. S. and Khadse, B. G. (2003). *Indian Drugs.* 40 (3) 147-150.

Mary, E. H., Gregory, B., Victor, N. and Adel, N. (2006). Pyrrolidine bis-cyclic guanidines with antimicrobial activity against drug-resistant Gram-positive pathogens identified from a mixture-based combinatorial library. *Bioorg. Med. Chem. Lett.* 16 5073-5079.

Matta, L. F. and Boyd, R. J. (2007). An Introduction of the Quantum theory of Atom in Molecule. *Wiley- VCH Verlag Gmbh*.

Mekala, R., Kamaraju, R., Regati, S., Gudimalla, N., Bannoath, C. K. and Sarva, J. (2016). A concise approach to substituted Quinazolin-4(3*H*)-one natural products catalyzed by Iron (III) Chloride. *Tetrahedron Letters* 57 1418–1420.

Parr, R. G., Szentpaly, L. and Liu, S. (1999). Electrophillicity Index. *J. Am. Chem. Soc*. 121 1922–1924.

Paytash, L. P., Sparrow, E. G. and Joseph, C. (1950). The reaction of itaconic acid with primary amine. *J. Am. Chem. Soc*. 72 1415-1416.

Prabavathi, N. and Nayaki, N. S. (2014). The spectroscopic (FT-IR, FT-Raman and NMR), first order hyperpolarizability and HOMO–LUMO analysis of 2-mercapto-4(3H)-quinazolinone. *Spectrochimica Acta Part A: Molecular and Biomolecular Spectroscopy* 129 572–583.

Prasad, M. V. S., Chaitanya, K., Udaya, Sri. N. and Veeraiah, V. (2013). Experimental and theoretical (HOMO, LUMO, NBO analysis and NLO properties) study of 7-hydroxy-4-phenylcoumarin and 5, 7-dihydroxy-4-phenylcoumarin. *Journal of Molecular Structure* 1047, 216–228.

Reed, A. E., Curtis, L. A. and Weinhold, F. (1988). Intermolecular interactions from a natural bond orbital, donor-acceptor viewpoint. *Chem. Rev.* 88 899–926.

Roeges, N. P. G. (1994). A Guide to the Complete Interpretation of the Infrared Spectra of Organic Structures. New York: *Wiley*.

Roja, G., Vikrant, B. H., Santosh, K. S., Asmita, S. and Pushpa, K. K. (2011). Accumulation of Vasicine and vasicinone in tissue cultures of Adhatoda vasica and evaluation of the free radical-scavenging activities of the various crude extracts. *Food Chemistry* 126 1033–1038.

Rozas, I., Alkorta, I. and Elguero, J. (2000). Behavior of Ylides Containing N, O, and C Atoms as Hydrogen Bond Acceptors. *J. Am.Chem. Soc*. 122 11154-11161.

Sathyanarayana, D. N. (2004). New Delhi: *New Age International(P) Ltd. Publishers*.

Sethi, A. and Prakash, R. (2015). Novel synthetic ester of Brassicasterol, DFT investigation including NBO, NLO response, reactivity descriptor and its intramolecular interactions analyzed by AIM**.** *Journal of Molecular Structure* 1083, 72–81.

Shinichi, I., Yuji, I., Taeko, H., Osamu, K., Yoshihiro, M., Yoshihiro, S., Naoyuki, K., Yuji, I., Masanori, B. and Shohei, H. (2004). CCR5 Antagonists as Anti-HIV-1 Agents. 1. Synthesis and Biological Evaluation of 5-Oxopyrrolidine-3-carboxamide Derivatives. *Chem. Pharm. Bull.* 52(1) 63-73.

Silverstein, R. M. and Webster, F. X. (2003). Spectrometric Identification of Organic Compounds. sixth ed. Asia: *John Wiley*.

Singh, R. N., Kumar, A., Tiwari, R. K. and Rawat, P. (2013). Synthesis, molecular structure, hydrogen-bonding, NBO and chemical reactivity analysis of a novel 1, 9-bis (2-cyano-2-ethoxycarbonylvinyl)-5-(4-hydroxyphenyl)-dipyrromethane: A combined experimental and theoretical (DFT and QTAIM) approach. *Spectrochimica Acta Part A: Molecular and Biomolecular Spectroscopy* 113 378–385.

Soliman, S. M., Hagar, M., Ibid, F., Sayed, E. and Ashry, H. E. (2015). Experimental and theoretical spectroscopic studies, HOMO–LUMO, NBO analyses and thione–thiol tautomerism of a new hybrid of 1, 3, 4-oxadiazole-thione with quinazolin-4-one**.** *Spectrochimica Acta Part: A Molecular and Biomolecular Spectroscopy* 145 270–279.

Schlegel, H. B. (1982). Optimization of equilibrium geometries and transition structures. *J. Comput. Chem*. 3 214-218.

Tran, J. A., Chen, C. W., Jiang, W., Tucci, F. C., Fleck, B. A., Marinkovic, D., Arellano, M. and Chen, C. (2007). Pyrollidines as potent functional agonists of the human melanocortin-4 receptor. *Bioorg. Med. Chem. Lett.* 17 5165-5170.

Wolinski, K., Hinton, J. F. and Pulay, P. (1990). Efficient implementation of the gauge-independent atomic orbital method for NMR chemical shift calculations. *J. Am. Chem. Soc.* 112 8251-8260.

Xun Li, Yalin Li and Wenfang Xu (2006). Design, synthesis, and evaluation of novel galloyl pyrrolidine derivatives as potential anti-tumor agents. *Bioorg. Med. Chem.* 14 1287-1293.

Zaater, S., Bouchoucha, A., Djebbar, S. and Brahimi, M. (2016). Structure, vibrational analysis, electronic properties and chemical reactivity of two benzoxazole derivatives: Functional density theory study. *Journal of Molecular Structure*, 1123, 344–354.

Corresponding author: Dr. Abha Bishnoi, Professor, Department of Chemistry, University of Lucknow, Lucknow-226007, India.
Email - abhabishnoi5@gmail.com, dr.abhabishnoi@gmail.com, hudaimranbeg@gmail.com
Phone - +91-9415028822, +91-7081165514